Evolving Design and Mobility of a Spacecraft on Stilts to Explore Asteroids

Article *in* Advances in the Astronautical Sciences · January 2020

Himangshu Kalita
The University of Arizona

E. Asphaug
Arizona State University

Jekan Thangavelautham
The University of Arizona

(Preprint) AAS XX-XXX

EVOLVING DESIGN AND MOBILITY OF A SPACECRAFT ON STILTS TO EXPLORE ASTEROIDS

Himangshu Kalita,[*] Felicity Aldava,[†]
Erik Asphaug [‡] and Jekan Thangavelautham[§]

Exploration of asteroids and comets will help to answer fundamental questions about the origins of the solar system. There are estimated to be nearly 2 million asteroid and comets in the solar system, and they are strategic locations for planetary science, planetary defense/security and for resource mining. Landing on these small bodies and manipulating their surface remains a major technical challenge fraught with high risk. The low gravity and low cohesive forces holding dust, gravel, and boulders together could result in surface ranging from 'quicksand' to a hard gravel surface. The latest asteroid missions such as Hayabusa II and OSIRIS-REx will perform touch and go operations to mitigate the risks of 'landing' on an asteroid. Beyond these missions, there is an important need to perform surface and subsurface sampling from multiple points on an asteroid. The SPIKE (Spacecraft Penetrator for Increasing Knowledge of NEOs) spacecraft architecture is unique in that it is a hybrid combination of an orbiter and lander. The spacecraft extends out a low-mass, high-strength boom that has a series of in-situ instruments at the tip to sample the surface and subsurface of the asteroid from a distance. In this paper, we extended the design of the SPIKE spacecraft concept into two booms with each boom consisting of three revolute joints. By utilizing the latest advances in automated computer design the trajectories of each joint are optimized such that the spacecraft can perform multiple hops and walks on an asteroid surface. There however remain uncertainties with the asteroid surface material, hardness and overall risk posture on the mission. Using this proposed design, we attempted to refine our preliminary landing system. The proposed spacecraft design and controls approach is a major departure from conventional spacecraft with amphibious capabilities of a lander and orbiter vehicle packaged in one.

INTRODUCTION

There are one million asteroids larger than 40 m diameter, and about a thousand bigger than 1 km. Asteroids are diverse in physical and dynamical properties and composition. They are time capsules of the early solar system and the planet formation processes. Many are resource-rich containing water, carbon-compounds, iron and platinum group metals. These small bodies are remnants of planet formation, progenitors of meteorites, and are therefore high-value targets identified

[*] Ph.D. Candidate, Aerospace and Mechanical Engineering, University of Arizona, Tucson AZ 85721.
[†] Undergraduate Student, Department of Computer Science, University of Arizona, Tucson AZ 85721.
[‡] Professor, Lunar and Planetary Laboratory, University of Arizona, Tucson AZ 85721.
[§§] Assistant Professor, Aerospace and Mechanical Engineering, University of Arizona, Tucson AZ 85721.

in the Planetary Science Decadal Survey. Some of these asteroids are potential hazards that may impact Earth.

Asteroid surfaces may contain everything from hard boulders to soft regolith that is loosely held by cohesion and low gravity. Their global structure may be that of a rubble pile [1] or a fractured monolith, with a tendency of coarser and fewer loose materials as one goes to smaller and smaller size [2]. The unknowns are as basic as if the asteroid behaves as a rigid surface or quicksand [3]. Upcoming and ongoing missions to asteroids such as Hayabusa II [4] and OSIRIS-Rex [5] will perform touch and go operations to mitigate the risks of 'landing' on an asteroid. This limits the contact time with the asteroid and requires significant fuel expenditure for hovering. Landing on a small asteroid and manipulating its surface contents remains a major unsolved challenge fraught with high risk [6,7]. It is a critical engineering challenge that needs to be solved to make surface exploration, resource mining and ambitious plans to setup communication relays and observatories possible. The extremely low gravity of these smaller asteroids offers some unique opportunities, leading to our proposed approach of a spacecraft on one or more stilts. Stilts may allow hopping on and or off the asteroid using very little energy, eliminating or minimizing the need for combustible chemical propulsion. Instead, conventional electrical thrusters with milli-newtons of thrust might be sufficient to propel on and off small asteroids, especially if a hopping force can be applied by the stilt. This translates into significant cost and risk reduction. This approach opens the opportunity of touching down and visiting multiples sites on an asteroid. Even more ambitious is the possibility of performing subsurface measurements.

We have proposed Spacecraft Penetrator for Increasing Knowledge of NEOs (SPIKE) [8,9], an ESPA-class solar electric propulsion (SEP) spacecraft. SPIKE is a unique amphibious, lander/flyby spacecraft that would perform multiple landings on an asteroid. It would perform in-situ analysis of the surface and subsurface regolith, in addition to seismic measurements to provide insight on the internal physical structure of the asteroid. The spacecraft touches the asteroid from a probing distance, utilizing an extended boom with science instruments mounted on the tip. Unlike a compact lander [9,10], SPIKE can depart the asteroid after it has completed its science objectives, and with sufficient fuel, can perform tours to multiple asteroid destinations.

In this paper, we extended the design of the SPIKE spacecraft concept into two booms with each boom consisting of three revolute joints. We present a dynamics model of the proposed SPIKE spacecraft concept for simulations. The dynamics model is then used to find optimized trajectories of each joint such that the spacecraft can perform multiple hops and walks on an asteroid surface using Evolutionary Algorithms. The preliminary results show that the motion of the spacecraft evolved into a hybrid hopping/walking pattern.

MISSION CONCEPT

SPIKE is an amphibious lander/flyby spacecraft propelled using xenon fueled solar-electric Hall thrusters. The onboard instruments would be used to analyze subsurface volatiles and organics and for conducting seismology on asteroids. A potential spacecraft design is based on the JPL Micro Surveyor that has a mass of 75 kg (wet). The science payload will include seismometers, cameras and other instruments that will be designed to access >10 cm beneath the surface of the asteroid. Power is provided by two sets of independently gimballed triple junction solar panels that generate 4 750 W and a Lithium Ion main battery of 2 kWh. The spacecraft utilizes electric propulsion using Hall Thrusters (JPL MasMi) fueled using Xenon. The spacecraft is estimated to have a delta-V of 5 km/s. The thrusters will be gimballed to desaturate the onboard reaction wheels and to perform landing and take-off maneuvers from the asteroid. The spacecraft attitude determination and control system will utilize Blue Canyon's XACT 50 that includes an integrated start-tracker, IMU and 3 reaction wheels. For communications, it will include JPL's DSN compatible IRIS X-band Radio V2.1 that will permit up to 256 KBps with a rigid 0.3 m parabolic dish. Moreover, the spacecraft has a 3 m rigid deployable truss which holds the science instrument module as shown in Figure 1.

The science mission begins with a survey phase using a camera to determine asteroid rotation state and gravity, and other dynamical characteristics, and to search for the suitable landing sites: regions with regolith, preferably that have been in seasonal shadow for some time as shown in Figure 2 (Concept of Operations). The spacecraft then descends in a precisely guided free-fall, impacting slowly while deploying the extendable boom. The bus comes to rest vertically on top of the science instrument module, deployed at the end of the truss. The base has two penetrators that are pushed into the subsurface to perform science operations. When science operations are complete, the spacecraft disengages by vibrating the regolith to break any cohesion and hops with an initial velocity > 1cm/s. The spacecraft then gets ready to land at a new regolith patch, in another guided free-fall. This is done repeatedly and after the first asteroid investigation is complete, SPIKE travels to a second NEO, and possibly a third.

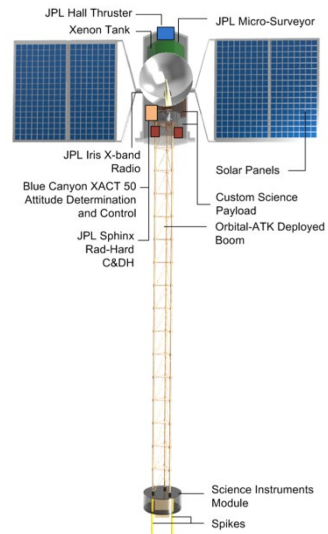

Figure 1: SPIKE concept

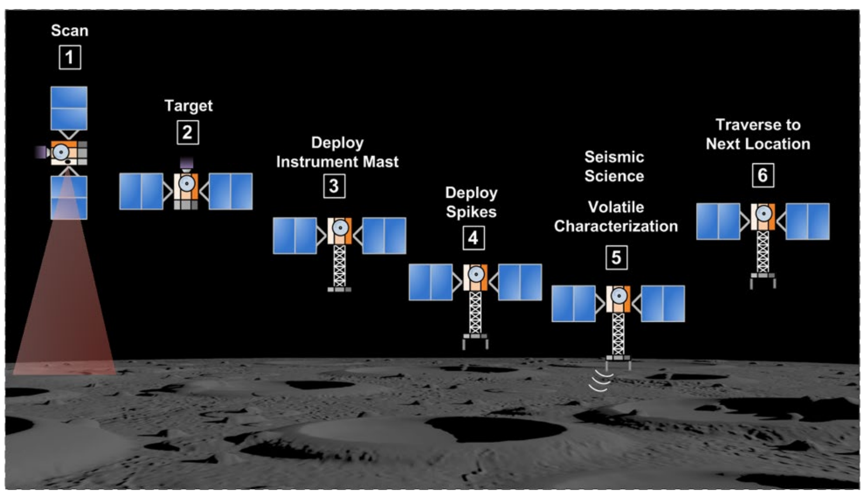

Figure 2: SPIKE Concept of Operation

Although the generalized design of SPIKE consists of one boom, we extend its design to two booms, each consisting of three links connected through revolute joints for it to walk on the surface of a target asteroid. Thus, the system is modeled as consisting of 7 links with homogenous density in the form of a torso (spacecraft body) and two legs (booms); each leg composed of two links and one foot as shown in Figure 3. The six joints (2 ankles, 2 knees, and 2 hips) are one-degree-of-freedom rotational frictionless joints. Additionally, we assume that the bipedal walking trajectory consists of two phases: a fully actuated single-support phase (satellite standing on one boom) and an instantaneous double-support phase (both feet of both boom on the ground). During the single-support phase, the stance boom remains on the ground without slipping and in each step the swing boom moves forward from behind the stance boom to the front.

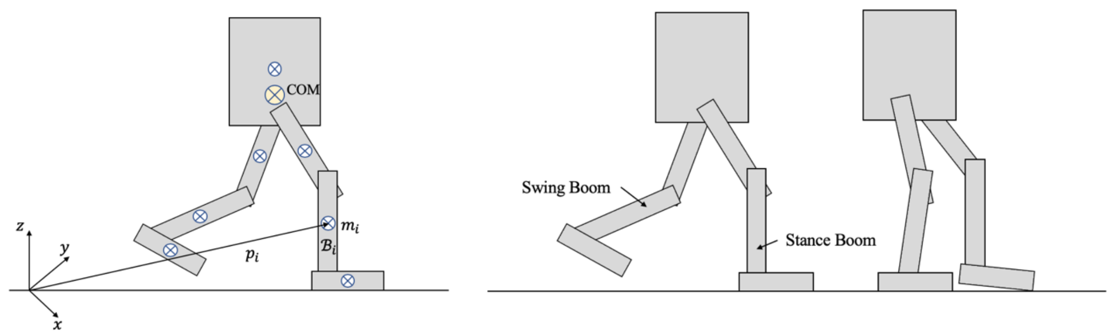

Figure 3: (Left) Schematic of the spacecraft model with two booms, (Right) Schematic of the single-support phase and double-support phase.

MODELING

In this section, the details of the dynamic model of the satellite with 2 booms is presented. The model is developed in two parts: first, the dynamics in the single-support phase is modeled by a set of differential equations with inputs, which are obtained from the Euler-Lagrange formulation. Second, a model of the collision of the swing foot and the ground is added to the Euler-Lagrange dynamics model [10].

Lagrangian Dynamics of the Satellite

With the 7-link bipedal model described in the previous section, let $\mathbb{p} := (p_1, \dots, p_7)$ denote the position, $\Theta := (\theta_1, \dots, \theta_7)$ denote the orientation of each link $\mathcal{B}_i$ and $\Gamma := (\tau_1, \dots, \tau_6)$ denote the input torques at each joint. Let us consider a vector of generalized coordinated $\mathbb{q} := (\mathbb{p}, \Theta)$, which represents the satellite's configuration. The Euler-Lagrange equations can be written as Eq. (1)

$$\frac{d}{dt}\frac{\partial \mathcal{L}}{\partial \dot{\mathbb{q}}_i} - \frac{\partial \mathcal{L}}{\partial \mathbb{q}_i} = \mu_i \tag{1}$$

Where, $\mathcal{L}(\mathbb{q}, \dot{\mathbb{q}}) := \mathcal{K}(\mathbb{q}, \dot{\mathbb{q}}) - \mathcal{P}(\mathbb{q})$ is the difference between the kinetic energy $\mathcal{K}$ and the potential energy $\mathcal{P}$ due to the gravity force; μ_i is the generalized force for each link. The kinetic energy and the potential energy are given by Eq. (2) and (3).

$$\mathcal{K}(\mathbb{q}, \dot{\mathbb{q}}) = \sum_{i=1}^{7} \left(\frac{1}{2} m_i \dot{p}_i^T \dot{p}_i + \frac{1}{2} J_i \dot{\theta}_i^2 \right) \tag{2}$$

$$\mathcal{P}(\mathbb{q}) = -\sum_{i=1}^{7} (m_i \mathbb{g}^T p_i) \tag{3}$$

Where, J_i is the moment of inertia of each link and $\mathbb{g} = (0,0,-g_z)$ is the gravity vector. The Euler-Lagrange equation for the system can be expressed in the second-order form as Eq. (4)

$$\mathbb{B}(\mathbb{q})\ddot{\mathbb{q}} + \mathbb{C}(\mathbb{q}, \dot{\mathbb{q}})\dot{\mathbb{q}} + \mathbb{G}(\mathbb{q}) = \mathbb{A}\Gamma \tag{4}$$

Where, $\mathbb{B}(\mathbb{q})$ is a positive definite symmetric matrix, known as the inertia matrix, the vector fields $\mathbb{C}(\mathbb{q}, \dot{\mathbb{q}})$ and $\mathbb{G}(\mathbb{q})$ include the centrifugal, Coriolis, and gravitational effects on the system, and the matrix $\mathbb{A}$ relates Γ with the vector of generalized forces μ. The model can then be expressed in a state-space form as Eq. (5)

$$\frac{d}{dt}\mathbb{x} = \begin{bmatrix} \dot{\mathbb{q}} \\ \mathbb{B}^{-1}(\mathbb{q})\left(\mathbb{u} - \mathbb{C}(\mathbb{q}, \dot{\mathbb{q}})\dot{\mathbb{q}} - \mathbb{G}(\mathbb{q})\right) \end{bmatrix} = f(\mathbb{x}) + g(\mathbb{x})\mathbb{u} \tag{5}$$

Where, $\mathbb{x} \coloneqq (\mathbb{q}, \dot{\mathbb{q}})$ is the state vector and $\mathbb{u} \coloneqq \mathbb{A}\tau = \mu$ is the control input.

Collision Model

The instantaneous double-support phase is modeled as a collision between the swing boom and the ground. The contact of the swing boom with the ground can be modeled by the application of a distribution of forces on the foot. For simplicity, we consider one resultant force and a corresponding torque both acting on the swing foot's ankle at the instant of contact. The effect of the impulsive external forces due to the collision is introduced as Eq. (6)

$$\mathbb{B}(\mathbb{q})\ddot{\mathbb{q}} + \mathbb{C}(\mathbb{q}, \dot{\mathbb{q}})\dot{\mathbb{q}} + \mathbb{G}(\mathbb{q}) = \mathbb{A}\tau + \mathbb{A}_F F_c + \mathbb{A}_\tau \tau_c \tag{6}$$

Where, F_c and τ_c are the resultant force and torque due to collision and $\mathbb{A}_F$ and $\mathbb{A}_\tau$ relates F_c and $\tau_c$with the vector of generalized forces μ. To calculate the collision forces between the swing boom and the ground, we implemented the Hertz contact force model and Coulomb's law of dry friction. When two bodies collide, local deformations occur resulting in penetration into each other's space. The penetration results in a pair of resistive contact forces acting on the two bodies in opposite directions. Every collision consists of a compression phase and a restitution phase which can be modeled as a non-linear spring-damper as shown in Eq. (7).

$$f_N = K\delta^n + d_c\dot{\delta} \tag{7}$$

where, K is the stiffness parameter, which depends on the material properties and the local geometry of the contacting bodies, δ is the penetration depth, d_c is the damping coefficient, $\dot{\delta}$ is the relative velocity of the contact points, projected on an axis normal to the contact surfaces and $n = 3/2$. For two colliding spheres with radii R_i and R_j, the parameter K can be determined as Eq. (8) and (9).

$$K = \frac{4}{3\pi\left(h_i + h_j\right)}\left(\frac{R_i R_j}{R_i + R_j}\right)^{\frac{1}{2}} \tag{8}$$

$$h_i = \frac{1 - v_k^2}{\pi E_k}; \;\; k = i, j \tag{9}$$

where, $v_k$and E_k are the Poisson's ratio and Young's modulus of each sphere. Also, the damping coefficient d_c can be considered as a function of the penetration depth, δ and the hysteresis damping factor, μ as shown in Eq. (10) and (11).

$$d_c = \mu\delta^n \tag{10}$$

$$\mu = \frac{3K(1 - e^2)}{4\,{}^{(-)}\dot{\delta}} \tag{11}$$

where, e is the coefficient of restitution and ${}^{(-)}\dot{\delta}$ is the penetration speed at the start of the compression phase. Each collision between the swing boom and the ground also results in a tangential frictional component of contact force which is computed using Coulomb's law of dry friction which opposes the relative motion. It has been experimentally found that the transition of friction force from zero to nonzero relative velocity is not instantaneous, but it takes place during a short period of time. This transition called the Stribeck effect is implemented to the equations of motion of the multibody system using the Anderson function to avoid stiction as shown in Eq. (12).

$$f_t = f_N \left(\mu_d + (\mu_s - \mu_d) e^{-\left(\frac{v_{i,j}}{v_s}\right)^p} \right) \tanh\left(k_t v_{i,j}\right) \tag{12}$$

where, μ_s is the coefficient of static friction, μ_d is the coefficient of dynamic friction, $v_{i,j} = v_i - v_j$ is the relative speed, v_s is the coefficient of sliding speed that changes the shape of the decay in the Stribeck region, exponent p affects the drop from static to dynamic friction and the parameter k_t adjusts the slope of the curve from zero relative speed to the maximum static friction. With the normal and tangential collision forces determined, the resultant force F_c is their vector sum.

Controller Design

Given the reference joint trajectories Θ_r for the six joints, we implement a closed-loop proportional-integral-derivative (PID) controller to calculate the joint torques as:

$$\Gamma = K_P e + K_D \dot{e} + K_I \int e \, dt \tag{13}$$

Where, $e = \Theta_r - \Theta$ is the error between the reference and actual joint trajectories, and K_P, K_D and $K_I$are positive definite matrices, typically diagonal that guarantee that $e \to 0$ as $t \to \infty$.

TRAJECTORY EVOLUTION

The objective is to find the optimal reference joint trajectories of the satellite booms such that its performance is maximized. The performance of the satellite is expressed as a fitness function $\mathcal{J}(\mathcal{G})$, where the reference joint trajectories Θ_r are encoded in the form of genes $\mathcal{G}$ for each joint as shown in Figure 4. Considering the gait period to be t_g, we define n number of trajectory point for each joint which are evenly space within time t_g. Moreover, the joint trajectories of the left leg are identical to the right leg, as such each gene is described by a $3 \times n$ matrix as shown in Table 1. Next the evenly space joint trajectories encoded as genes are converted into smooth trajectories using a third-order polynomial function as shown in Figure 6(Left). These smooth trajectories are the reference joint trajectories Θ_r. The PID controller calculates the input torque for each joint based on the reference joint trajectories Θ_r and feedback from dynamics model. The simulation is run for a time t_s and the position $\mathbb{p}$, velocity $\dot{\mathbb{p}}$ vectors of each link along with the input torque at each joint are used to calculate the fitness function $\mathcal{J}(\mathcal{G})$.

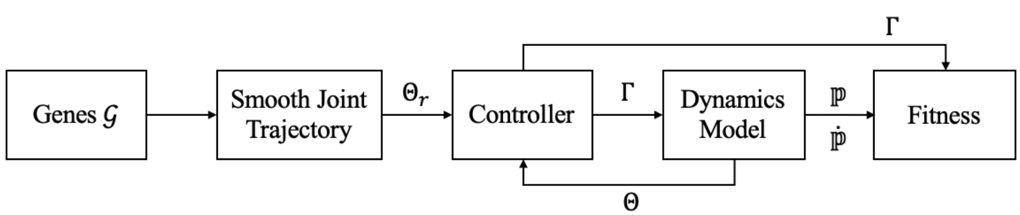

Figure 4: Block diagram for calculating the fitness function $\mathcal{J}(\mathcal{G})$ from the genes $\mathcal{G}$.

Table 1: Structure of each gene that defines the reference joint trajectories.

	$t=0$	t_g/n	$2t_g/n$	$3t_g/n$	…	$(n-1)t_g/n$
Hip	h_0	h_1	h_2	h_3	…	h_{n-1}
Knee	k_0	k_1	k_2	k_3	…	k_{n-1}
Ankle	a_0	a_1	a_2	a_3	…	a_{n-1}

The performance of the satellite is measured against three parameters: 1) Distance travelled without falling, 2) Simulation time without falling, and 3) Input torques at each joint. The objective is to increase the distance travelled and simulation time without falling and decrease the input torques at each joint, as such the fitness function is defined as Eq. (14).

$$\mathcal{J}(\mathcal{G}) = -\frac{\left(\mathbb{p}_{y(COM)}(t_s)\right)^2 t_s}{\sum_{i=1}^{3} \int \tau_i \, dt} \tag{14}$$

where, $\mathbb{p}_{y(COM)}(t_s)$ is the position of the center of mass of the entire system at the end of the simulation in the y-direction (direction of motion). Moreover, since the escape velocity on asteroid surfaces are extremely low, we add a constraint such the velocity of the center of mass of the system, $||\dot{\mathbb{p}}_{COM}||$ is less than the escape velocity v_{esc} of the target body. The optimization problem can then be mathematically expressed as Eq. (15).

$$\begin{aligned} &\min_{\mathcal{G}} \mathcal{J}(\mathcal{G}) \\ s.t.\ \ & g(\mathcal{G}) \equiv ||\dot{\mathbb{p}}_{COM}|| < v_{esc} \end{aligned} \tag{15}$$

With the optimization problem defined, the penalty function approach is used to handle the constraint with the objective function. We then use an Evolutionary Algorithm approach to solve for the optimization problem. First an initial population P_0 is created by generating N random individuals. Then, the usual tournament selection, crossover, and mutation operators are used to create an offspring population Q_0 of size N_Q. For crossover, we perform a single-point crossover operator on the two individuals selected for mating. For mutation, we use a gaussian mutation operator where the selected element of an individual is replaced with a value generated by a gaussian process. Elitism is introduced by comparing the current population with previously found best solutions. For the t^{th} generation, first a combined population $R_t = P_t + Q_t$ is formed. The population R_t is of size $N + N_Q$. Since all previous and current population members are included in R_t, elitism is ensured. Next, the fitness of each individual in R_t is calculated according to the cost function $\mathcal{J}(\mathcal{G})$. Based on the value of the cost function, the population is sorted in ascending order and the best N individuals are selected for the next generation. The new population P_{t+1} of size N is again used for selection, crossover, and mutation to create a new population Q_{t+1} of size N_Q. The process is repeated until desired results are obtained, or the maximum number of generations is achieved.

RESULTS

The simulations were performed with total mass of the spacecraft $m = 75$kg, gravity $g_z = 0.2$m/s^2, and the length of the two links of each boom as 0.4m. The evolutionary algorithm was run for 150 generations with 100 individuals in each generation. Figure 6(Right) shows the best and mean fitness in each generation. It can be seen that the fitness function improved with generations. The model of the spacecraft with the two booms is developed using MATLAB Simulink and Simscape environments. Figure 5 shows a few snapshots of the spacecraft walking using the two booms.

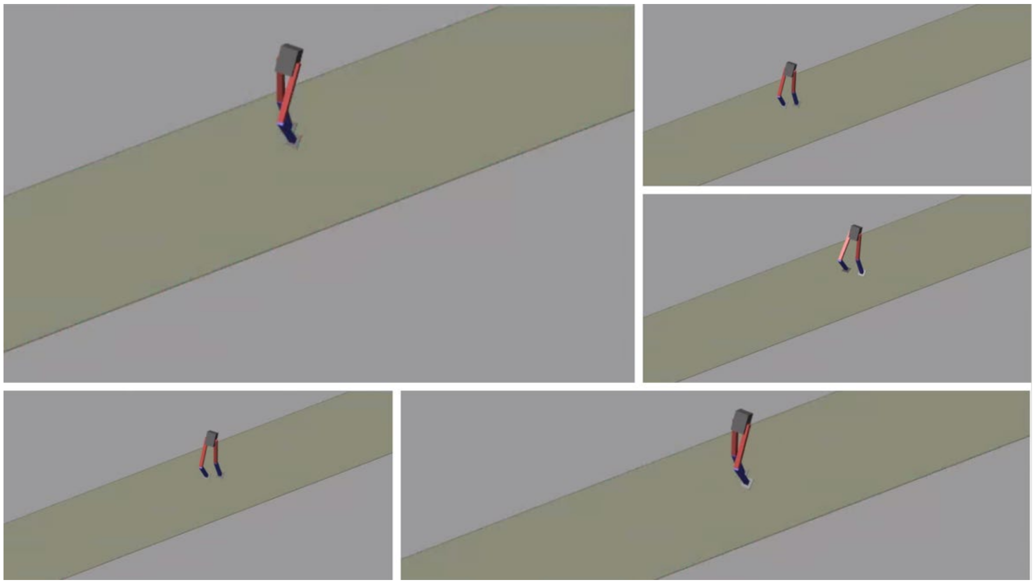

Figure 5: Snapshots of the dynamic simulation of the spacecraft on two booms.

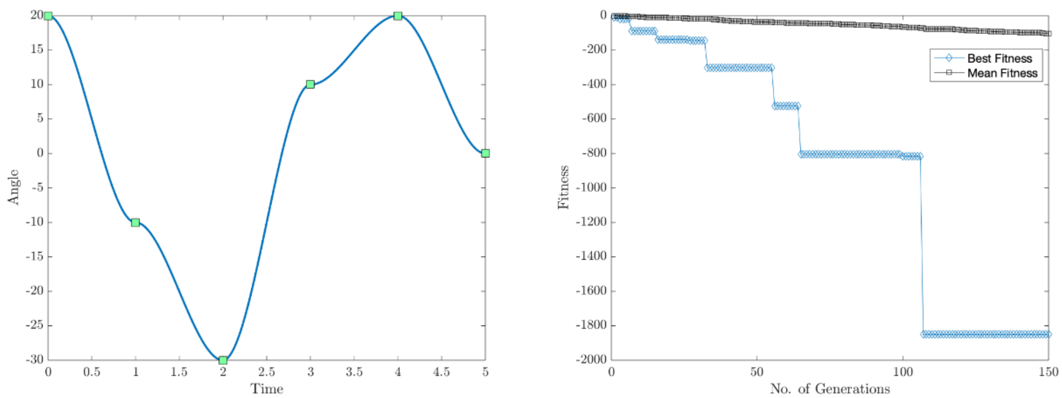

Figure 6: (Left) Cubic polynomial generated from 6 evenly spaced trajectory points to find the reference joint trajectories from each gene, (Right) Best and mean fitness over number of generations.

Figure 7(Top-Left) shows the position of the center of mass of the spacecraft body along x, y and z direction for the fittest individual. From the x and y positions, it can be seen that the spacecraft moved forward along y direction with minor deviations along x direction. The z position of the spacecraft shows that the motion of the spacecraft evolved into a hybrid hopping/walking pattern. Although, the simulation was performed for walking mobility, the hopping mobility was introduced due to the low gravity conditions of the asteroid. The joint angles and joint torques for the fittest individual are shown for the hip joint (Figure 7(Top-Right)), knee joint (Figure 7(Bottom-Left)), and ankle joint (Figure 7(Bottom-Right)).

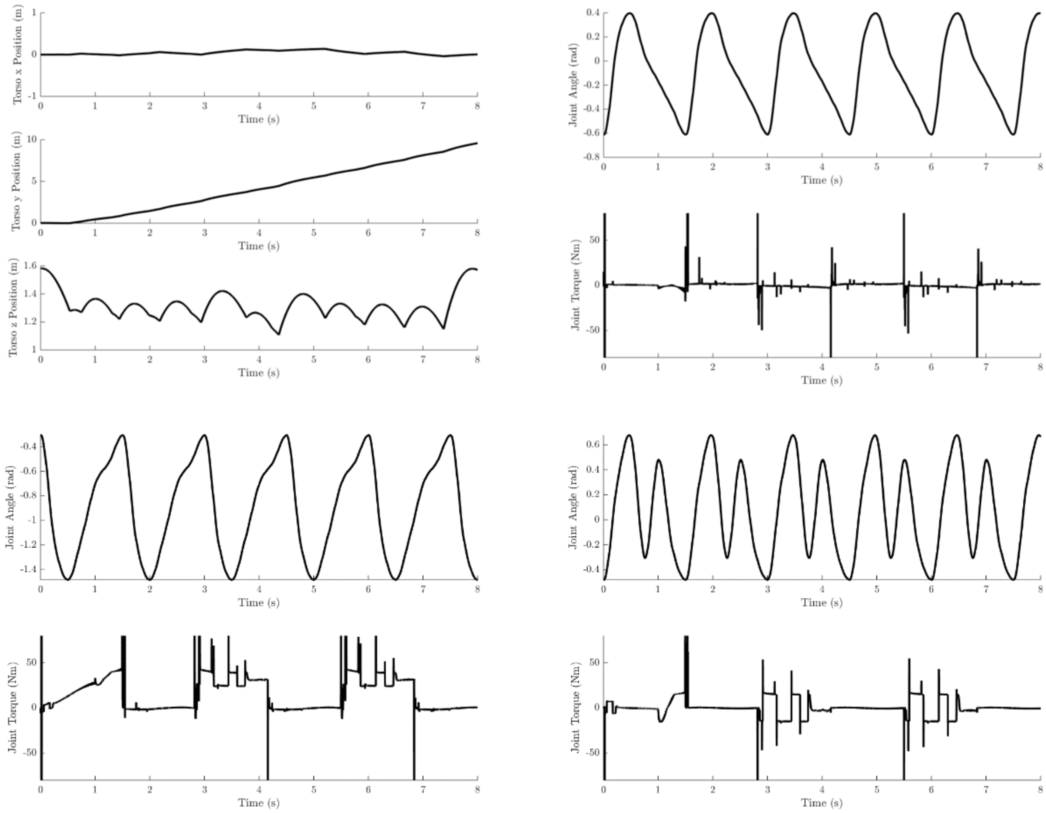

Figure 7: (Top-Left) Position of the center of mass of the spacecraft body along x, y and z direction for the fittest individual. Joint angle and joint torque of (Top-Right) Hip joint, (Bottom-Left) Knee joint, and (Bottom-Right) Ankle joint for the fittest individual.

CONCLUSION

In this paper we presented a unique spacecraft architecture, SPIKE (Spacecraft Penetrator for Increasing Knowledge of NEOs) that it is a hybrid combination of an orbiter and lander. The spacecraft extends out a low-mass, high-strength boom that has a series of in-situ instruments at the tip to sample the surface and subsurface of the asteroid from a distance. We extended the design of the spacecraft into two booms, with each boom consisting of three links connected through three one-degree-of-freedom revolute joints. The extension of the design into two booms allows it to perform multiple hops and walks on an asteroid surface. We presented a dynamics model of the spacecraft with the two booms and used the dynamics model to find optimal trajectories of each joint to perform walking on an asteroid surface. This is done through the use of Evolutionary Algorithms that uses the Darwinian theory of 'survival of the fittest' to find the fittest individual to perform the desired task. Our results show that the motion of the spacecraft evolved into a hybrid hopping/walking pattern due to the low gravity asteroid environment. Although the preliminary results show acceptable results, the paper leaves numerous important extensions that are under study and include finding optimal number and size of booms. The path forward shows a compelling, low-cost and innovative method for performing asteroid surface exploration.

ACKNOWLEDGMENTS

We would like to gratefully acknowledge Dr. Stephen Schwartz for helpful discussions.

REFERENCES

1. A. Fujiwara, et al., "The rubble-pile asteroid Itokawa as observed by Hayabusa." *Science*, 2006 Jun 2, 312(5778): 1330-4.
2. C. M. Hartzell, D. J. Scheeres, "Dynamics of levitating dust particles near asteroids and the Moon." *J. Geophys. Res. Planets*, 2013, 118, 116-126, doi:10.1029/2012JE004162.
3. E. Asphaug, "Growth and Evolution of Asteroids." *Annual Review of Earth and Planetary Sciences*, 2009 37:1, 413-448.
4. J. Kawaguchi, A. Fujiwara, T. Uesugi, "Hayabusa – Its technology and science accomplishment summary and Hayabusa 2." *Acta Astronautica* 62 (2008) 639-647.
5. D. S. Lauretta, et al., "OSIRIS-Rex: Sample Return from Asteroid." *Space Science Reviews*, 2017.
6. H. Kalita, E. Asphaug, S. Schwartz, J. Thangavelautham, "Network of Nano-Landers for In-Situ characterization of asteroid impact studies." *68th International Astronautical Congress (IAC)*, Australia, 2017.
7. H. Kalita, A. Ravindran, J. Thangavelautham, "Exploration and Utilization of Asteroids as Interplanetary Communication Relays." *IEEE Aerospace Conference*, 2018.
8. E. Asphaug, et al., "Spacecraft penetrator for increasing knowledge of NEOs (SPIKE)." *48th Lunar and Planetary Science Conference*, 2017.
9. H. Kalita, et al., "Mobility and Science Operations on an Asteroid using a Hopping Small Spacecraft on Stilts." *Advances in the Astronautical Sciences*, 2019.
10. J. E. Machado, et al., "Modeling and Finite-Time Walking Control of a Biped Robot with Feet," *Mathematical Problems in Engineering*, 2015.